Proceedings of the 3rd International Congress APMAS2013, April 24–28, 2013, Antalya, Turkey

Effects of RF Power on Electrical and Structural Properties of Sputtered SnO_2:Sb Thin Films

O. Cevher, M.O. Guler, U. Tocoglu, T. Cetinkaya, H. Akbulut and S.C. Okumus
Sakarya University, Engineering Faculty, Department of Metallurgical and Material Engineering
Esentepe Campus, Sakarya, Turkey

In this work, antimony doped tin oxide (SnO_2:Sb) thin films were fabricated using a radio frequency magnetron sputtering system on Si wafer and glass substrates. The base pressure in the sputtering chamber was 1.0 Pa. The SnO_2:Sb thin films were deposited for 1.0 h in a mixture of Ar and O_2 environment with O_2/Ar ratio of 10/90 at 75, 100, and 125 W RF sputtering powers. The microstructure of SnO_2:Sb thin films was assessed using a field emission scanning electron microscopy. The crystallographic structure of the sample was determined by X-ray diffraction. The average surface roughness (R_a) was measured with atomic force microscopy. The electrical resistivity of the deposited films was measured by the four-point-probe method. The thicknesses of the films were measured by surface profiler.

DOI: 10.12693/APhysPolA.125.293
PACS: 68.55.−a, 68.55.ag, 81.15.Cd

1. Introduction

The SnO_2 film is a transparent conductive coating material and an n-type semiconductor with a wide band gap (approximately 3.7 eV) [1] and has tetragonal rutile structure. The SnO_2 film shows the best thermal and chemical stability, it is inexpensive, and it has good adhesion to most of the substrates, but it has high resistivity. The optical band gap, resistivity, carrier type, and concentration of SnO_2 films can be easily adjusted with addition of a dopant. The most common dopants used for sputter deposited SnO_2 thin films are antimony (Sb) and indium (In) [2–4]. The SnO_2 films have great potential for application in various fields, such as gas sensors [5], solar cells [6], optoelectronic devices [7], flat panel displays [8], and heat mirrors [9].

The properties of the films are generally affected by preparation conditions such as deposition techniques, substrate temperature, working pressure, types of substrates and the thickness of the films [10]. The conductive antimony doped tin oxide (ATO) films are prepared by various methods such as chemical vapor deposition [11], spray pyrolysis [12], sputtering [13, 14], pulsed-laser deposition (PLD) [15] and dip coating [16]. RF magnetron sputtering is one of the most promising deposition techniques due to the advantages of low deposition temperature, simple processing, whilst yielding the preferred orientation and uniform properties [17], inexpensive equipment and suitability for large area deposition.

The aim of this paper is to investigate the effect of RF power on the structural and electrical properties of SnO_2:Sb thin films deposited on silicon wafer and glass substrates by RF magnetron sputtering technique. Our work tends to focus on the changes in the crystallinity, surface roughness, grain size, deposition rate and resistivity of SnO_2:Sb thin films as a result of RF power.

2. Experimental

The experimental process parameters used in this study are shown in Table. The SnO_2:Sb thin films were deposited on glass, silicon wafer and stainless steel substrates using RF magnetron sputtering. The target was an SnO_2:Sb disc (SnO_2:Sb = 90:10% in weight, purity 99.99%) of a diameter of 50.8 and 6.35 mm thick. The RF powers were 75, 100, and 125 W. The flow rate of Ar and O_2 gases was fixed by a TDZM-III mass flow controller. The substrate was not heated deliberately and not measured.

TABLE

Parameters of sputter deposition of the SnO_2:Sb thin films.

sputtering pressure	1.0 Pa
substrate	glass and silicon wafer
substrate temperature	room temperature
substrate to target distance	13.5 cm
deposition time	60 min
oxygen partial pressure $[(O_2/(O_2+Ar)]\cdot 100$	10%
RF power	75, 100, and 125 W

The crystalline structure of SnO_2:Sb thin films was characterized by X-ray diffraction (XRD) technique. The XRD patterns of the deposited SnO_2:Sb thin films were obtained by an X-ray diffractometer (Rigaku D/MAX 2000 with a multipurpose attachment) using Cu K_α radiation ($\lambda = 1.54056$ Å). The scan rate used was 2°/min and the scan range was from 10° to be 90°. The grain size as calculated by Scherrer's formula [17]:

$$D = \frac{0.9\lambda}{B\cos\theta},$$

where D is the mean grain size, λ is the X-ray wavelength, B is the corrected full-width at half maximum (FWHM) and θ is the Bragg angle.

The resistivity of the films was also measured. A resistance meter with a four-point probe (Lucas Labs Pro4-4000 probe) was used to measure the electrical resistivity of SnO_2:Sb thin films. The surface morphology

of SnO_2:Sb thin films was investigated by field emission scanning electron microscopy (FESEM) (JSM-6335F). The surface roughness of the films was measured using an atomic force microscope (AFM) (Ntegra). The thickness of the films was measured using a profilometer (KLA Tencor P-6).

3. Results and discussions

FESEM micrographs of SnO_2:Sb thin films deposited with various RF powers at 10% oxygen partial pressure were presented in Fig. 1. The SnO_2:Sb thin films have a relatively smooth and dense surface. Grain agglomerates were also observed. The results show that the nanosized SnO_2:Sb particles were obtained. The Si wafer substrates were covered with morphology like Volmer–Weber type growth (Fig. 1) at various RF powers.

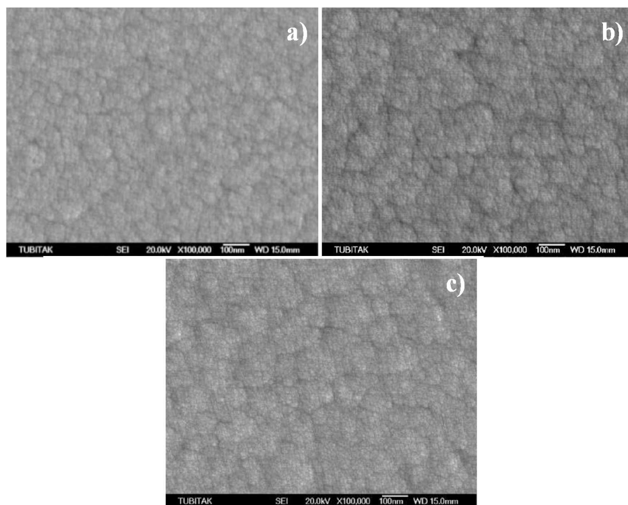

Fig. 1. FESEM micrographs of SnO_2:Sb thin films deposited at 10% oxygen partial pressure, (a) 75 W, (b) 100 W, and (c) 125 W RF powers.

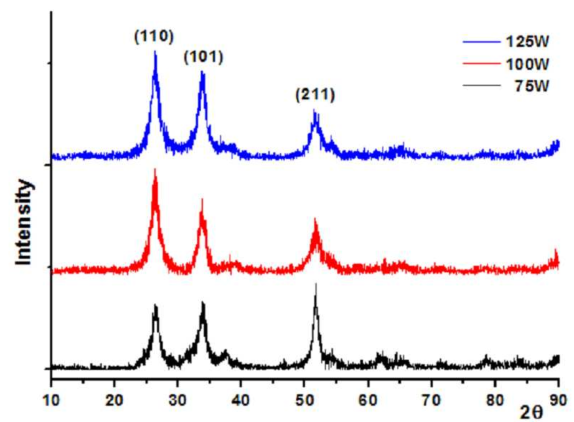

Fig. 2. X-ray diffraction patterns of the ATO thin films deposited with different RF powers at 10% oxygen partial pressure.

The crystallographic structure of SnO_2:Sb thin films deposited with different RF power at 10% oxygen partial pressure was presented in Fig. 2. The diffraction peaks indicate that tin oxide exists in cassiterite tetragonal (rutile type) structure (JCPDS card number 00-041-1445). The (110), (101) and (211) diffraction peaks were observed for SnO_2:Sb thin films deposited with different RF powers in 10% oxygen partial pressure. The intensity of peaks becomes more intense and sharper with the increase in RF power. This suggests that crystallinity of the resulting film increases with increasing RF power.

Figure 3 shows AFM micrographs of SnO_2:Sb thin films sputtered with various RF powers at 10% oxygen partial pressure.

The surface roughness of SnO_2:Sb thin films were also illustrated in Fig. 4. The roughness of SnO_2:Sb thin film increases from 3.516 to 4.778 nm with the increase of RF power from 75 W to 125 W. It is evident from the AFM micrograph that the growth of SnO_2:Sb thin films is in the columnar nature and grain size is increased by increasing RF power.

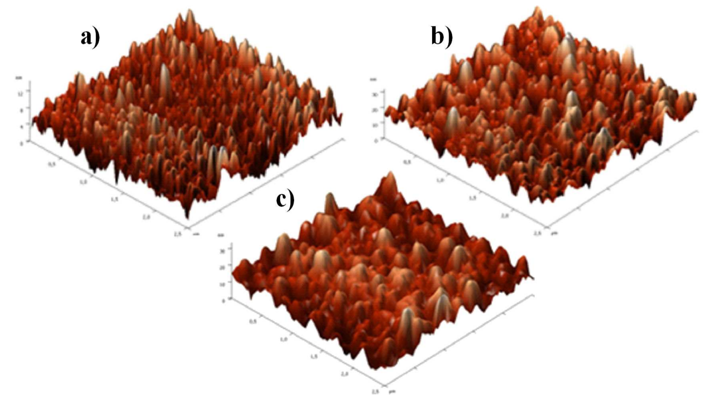

Fig. 3. AFM morphologies of SnO_2:Sb thin films deposited at 10% oxygen partial pressure, (a) 75 W, (b) 100 W, and (c) 125 W RF powers.

The deposition rate and grain size of SnO_2:Sb thin films deposited with different RF powers at 10% oxygen partial pressure are shown in Fig. 4. Deposition rate decreases with an increase in RF power at 10% oxygen partial pressure. As the RF power increased from 75 W to 125 W, the deposition rate of SnO_2:Sb thin films increased from 9.68 nm/min to 20.51 nm/min. This can be explained by the fact that the number of sputtered SnO molecules at the target surface increases owing to the enhancement of bombardment by Ar^+ ions as the RF power increases and the resulting deposition rate increases [14]. The grain size increases gradually with the RF power. When the RF power is about 75 W, the average grain size is about 9.7 nm, when RF power is increased to 125 W, the grains also increase to about 12.1 nm. From this result, the grain size was observed to get bigger with the increase in the RF power because the increased power caused an increase in the energy of the Ar^+ ions when

they collided with the target and then an increase in the surface mobility of the sputtered particles [14].

Figure 4 shows the resistivity of SnO_2:Sb thin films deposited at different RF powers at 10% oxygen partial pressure. As the RF power increased from 75 W to 125 W, the resistivity of SnO_2:Sb thin films deposited on the glass substrate decreased from 0.159 to 0.0177 Ω cm. This result was very consistent with the other results mentioned previously. That is, the crystallinity was enhanced with higher RF power for the film deposition.

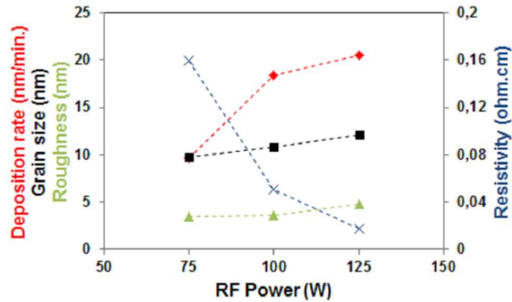

Fig. 4. Deposition rate, grain size, roughness, resistivity of SnO_2:Sb thin films deposited at 10% oxygen partial pressure and different RF powers.

4. Conclusions

Deposition rate increases with increased in the RF power. The intensity of peaks becomes more intense and sharper with the increase in RF power. The mean grain size increases with increased in the RF power. The average surface roughness of the film increases with the increased in the RF power. The electrical resistivity of SnO_2:Sb thin film decreases with increased in the RF power.

Acknowledgments

This work is supported by the Scientific and Technological Research Council of Turkey (TÜBİTAK) under the contract number 109M464. The authors thank the TÜBİTAK MAG workers for their financial support.

References

[1] F.J. Arlinghaus, *J. Phys. Chem. Solids* **35**, 931 (1974).

[2] K.Y. Rajpure, M.N. Kusumade, M.N. Neumann-Spallart, C.H. Bhosale, *Mater. Chem. Phys.* **64**, 184 (2000).

[3] T. Kawabe, S. Shimomura, T. Karasuda, K. Tabata, E. Suzuki, Y. Yamaguchi, *Surf. Sci.* **448**, 101 (2000).

[4] K.L. Chopra, S. Major, D.K. Pandya, *Thin Solid Films* **102**, 1 (1983).

[5] D. Haridas, K. Sreenivas, V. Gupta, *Sensors Actuat. B* **133**, 270 (2008).

[6] J.A. Ayllon, M. Lira-Cantu, *Appl. Phys. A* **95**, 249 (2009).

[7] R.E. Presley, C.L. Munsee, C.H. Park, D. Hong, J.F. Wager, D.A. Keszler, *J. Phys. D, Appl. Phys.* **37**, 2810 (2004).

[8] M.R. Cássia-Santos, V.C. Sousa, M.M. Oliveira, F.R. Sensato, W.K. Bacelar, J.W. Gomes, E. Longo, E.R. Leite, J.A. Varela, *Mater. Chem. Phys.* **90**, 1 (2005).

[9] G. Frank, E. Kaur, H. Kostlin, *Sol. Energy Mater.* **8**, 387 (1983).

[10] L.P. Peng, L. Fang, X.F. Yang, H.B. Ruan, Y.J. Li, Q.L. Huang, C.Y. Kong, *Physica E* **41**, 1819 (2009).

[11] J. Kane, H.P. Schweizer, W. Kern, *J. Electrochem. Soc.* **123**, 270 (1976).

[12] A.R. Babar, S.S. Shinde, A.V. Moholkar, C.H. Bhosale, J.H. Kim, K.Y. Rajpure, *J. Semicond.* **32**, 053001 (2011).

[13] H.L. Ma, X.T. Hao, J. Ma, Y.G. Yang, J. Huang, D.H. Zhang, X.G. Xu, *Appl. Surf. Sci.* **191**, 313 (2002).

[14] S.U. Lee, J.H. Boo, B. Hong, *Jpn. J. Appl. Phys.* **50**, 01AB10 (2011).

[15] H. Kim, A. Pique, *Appl. Phys. Lett.* **84**, 218 (2004).

[16] T.M. Hammad, N.K. Hejazy, *Int. Nano Lett.* **2**, 7 (2012).

[17] B.D. Cullity, *Elements of X-ray Diffraction*, Addison-Wesley, Massachusetts 1956.